Supplementary Information 2

Machine Learning Accelerated Discovery of High Transmittance in $(K_{0.5}Na_{0.5})NbO_3$-Based Ceramics

Bowen Ma,[1] Fangyuan Yu,[1] Ping Zhou, Xiao Wu,* Chunlin Zhao, Cong Lin, Min Gao, Tengfei Lin, Baisheng Sa*

College of Materials Science and Engineering, Fuzhou University, Fuzhou 350108, China.

*Correspondence author.

E-mail: wuxiao@fzu.edu.cn (X. Wu), bssa@fzu.edu.cn (B. Sa).

[1] Bowen Ma and Fangyuan Yu are contributed equally to the study.

1. Feature construction and selection

Supplementary Table 1. Original features in the feature pool for A-site and B-site elements.

Feature	Description
ST	Sintering temperature
MT_A	Melting point of A-site element[1]
MT_B	Melting point of B-site element
IR_A(Å)	Shannon's (1976) ionic radii of A-site (12-coordination) [2]
IR_B(Å)	Shannon's (1976) ionic radii of B-site (12-coordination)
AR_A(pm)	Atomic radius of A-site element [3]
AR_B(pm)	Atomic radius of B-site element
A-O(Å)	ideal A–O bond distance [4]
B-O(Å)	ideal B–O bond distance
V_A	Atomic volume of A-site element[1,5]
V_B	Atomic volume of B-site element
CVR_A	Crystallographic van der Waals radii of A-site element (S. S. Batsanov 2001) [6]
CVR_B	Crystallographic van der Waals radii of B-site element (S. S. Batsanov 2001)
EVR_A	Equilibrium van der Waals radii of A-site element (S. S. Batsanov 2001) [6]
EVR_B	Equilibrium van der Waals radii of B-site element
EP_A	Period of A-site element in element period table
EP_B	Period of B-site element in element period table
$CovR_A$(Å)	Covalent radii of A-site element [7]
$CovR_B$(Å)	Covalent radii of B-site element
Dve_A	Valence electron distance (Schubert) of A-site element[1]
Dve_B	Valence electron distance (Schubert) of B-site element
Dce_A	Core electron distance (Schubert) of A-site element[1]
Dce_B	Core electron distance (Schubert) of B-site element
M_A	Relative atomic mass of A-site element

M_B	Relative atomic mass of B-site element
NEC_A-S	Nuclear effective charge-Slater of A-site element[1]
NEC_B-S	Nuclear effective charge-Slater of B-site element
NEC_A-C	Nuclear effective charge-Clementi of A-site element[1]
NEC_B-C	Nuclear effective charge-Clementi of B-site element
AN_A	Atomic number of A-site element in element period table
AN_B	Atomic number of B-site element in element period table
Ven/NC-A	Ratio of valence electron number to nuclear charge of A-site element
Ven/NC-B	Ratio of valence electron number to nuclear charge of B-site element
P_A	Polarizability of A-site element [8,9]
P_B	Polarizability of B-site element
E_A-P	A-site electronegativity-Pauling scale[1]
E_B-P	B-site electronegativity-Pauling scale
E_A-MB	A-site electronegativity-Matyonov-Batsanov[1]
E_B-MB	B-site electronegativity-Matyonov-Batsanov
EI_A	First energy ionization of A-site element[5]
EI_B	First energy ionization of B-site element
EA_A	Electron affinity of A-site element[5]
EA_B	Electron affinity of B-site element
PCR_A	pseudopotential core radii of A-site element[10]
PCR_B	pseudopotential core radii of B-site element
C_A-a	Cell parameters of A-site element in the a direction[5]
C_B-a	Cell parameters of B-site element in the a direction
C_A-b	Cell parameters of A-site element in the b direction
C_B-b	Cell parameters of B-site element in the b direction
C_A-c	Cell parameters of A-site element in the c direction
C_B-c	Cell parameters of B-site element in the c direction
t	Tolerance factor calculated by Shannon's ionic radii
μ	Octahedral factor calculated by Shannon's ionic radii

Supplementary Table 1 shows the 27 initial features and 1 process parameter for the properties of perovskite A-site and B-site elements (atoms or ions) extracted from the literature and A. A. Baikov Institute of Metallurgy and Materials Science Database. We calculated the weighting of elements in the component to obtain the A-position and B-position feature features and define the material features as:

$$X_{A/B} = \frac{X_A}{X_B} = \frac{\sum_{i \in A} f_i X_i}{\sum_{i \in B} f_i X_i} \quad (1)$$

where f_i is the molar fraction and X_i is the elemental counterpart property. Combining with Supplementary Table 1 we obtained 20 material features. For ease of viewing, we removed the $X_{A/B}$ subscript and abbreviated it to an uppercase X.

The Pauling-electronegativity (E-P), Matyonov-Batsanov electronegativity (E-MB), first ionization energy (EI), electron affinity (EA) and pseudo-potential core radii (PCR) were mainly used to compare the difference between anions and cations, so we define it as:

$$X = |(X_A - X_O) + (X_B - X_O)|/2 \quad (2)$$

Tolerance factor *t* is an important parameter to demonstrate the stability of perovskite, which is defined as:

$$t = (R_A + R_0)/\sqrt{2}(R_B + R_0) \quad (3)$$

where R_A and R_B are the mole averaged ionic radius of the A-site and the B-site respectively, and R_0 is the ionic radius of the oxygen atom.

The octahedral factor (μ) is defined by:

$$\mu = R_B \,/\, R_0 \quad (4)$$

where R_B is the mole averaged ionic radius of the B-site and R_0 is the ionic radius of the oxygen ions.

The above generates a total of 28 features.

We grouped the features with Person correlation coefficients greater than 0.8 or less than -0.8. In each group, we chose a common feature related to the target property and represented the other features in the group. For example, in the first group of highly correlated Pauling-electronegativity (E-P), first energy ionization (EI), pseudopotential core radii (PCR), Octahedral factor (μ), Matyonov-Batsanov electronegativity (E-MB), we chose E-MB because of a common chemical property, and E-MB exhibited a higher correlation coefficient with *T*%. A total of 3 groups of highly relevant features were summarized and 3 features were retained, as shown in Supplementary Table 2.

Supplementary Table 2. Three groups of highly relevant features and the ones retained.

Highly relevant features	Retained feature within each group
E-P, EI, PCR, μ	E-MB
MT, IR, AR, X-O, CVR, EVR, EP, CovR, M, NEC-S, NEC-C, AN, P, C-a, C-b, t	Dce
V	Dve

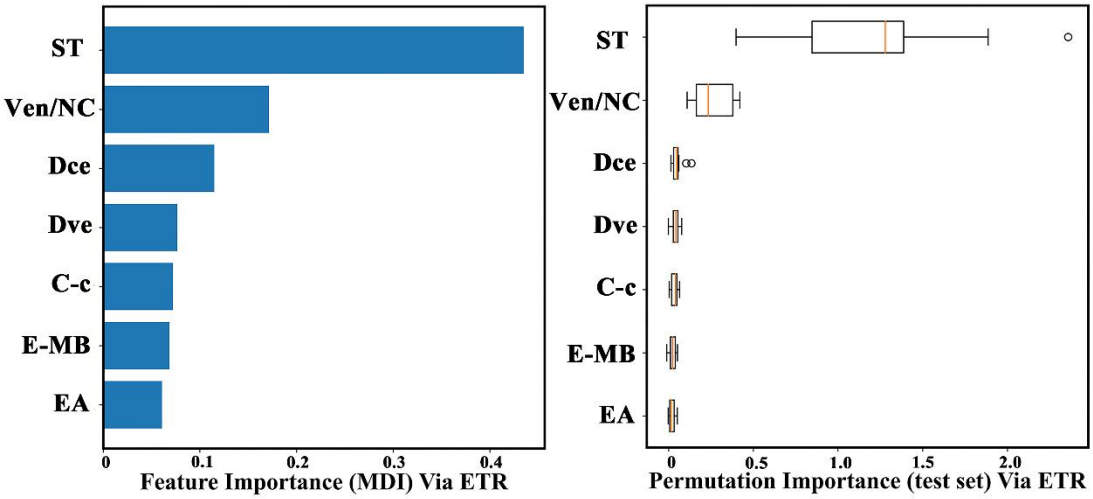

Supplementary Figure 1. Importance assessment of 7 features based on ETR model using Mean Decrease Impurity (MDI) and Permutation Importance methods.

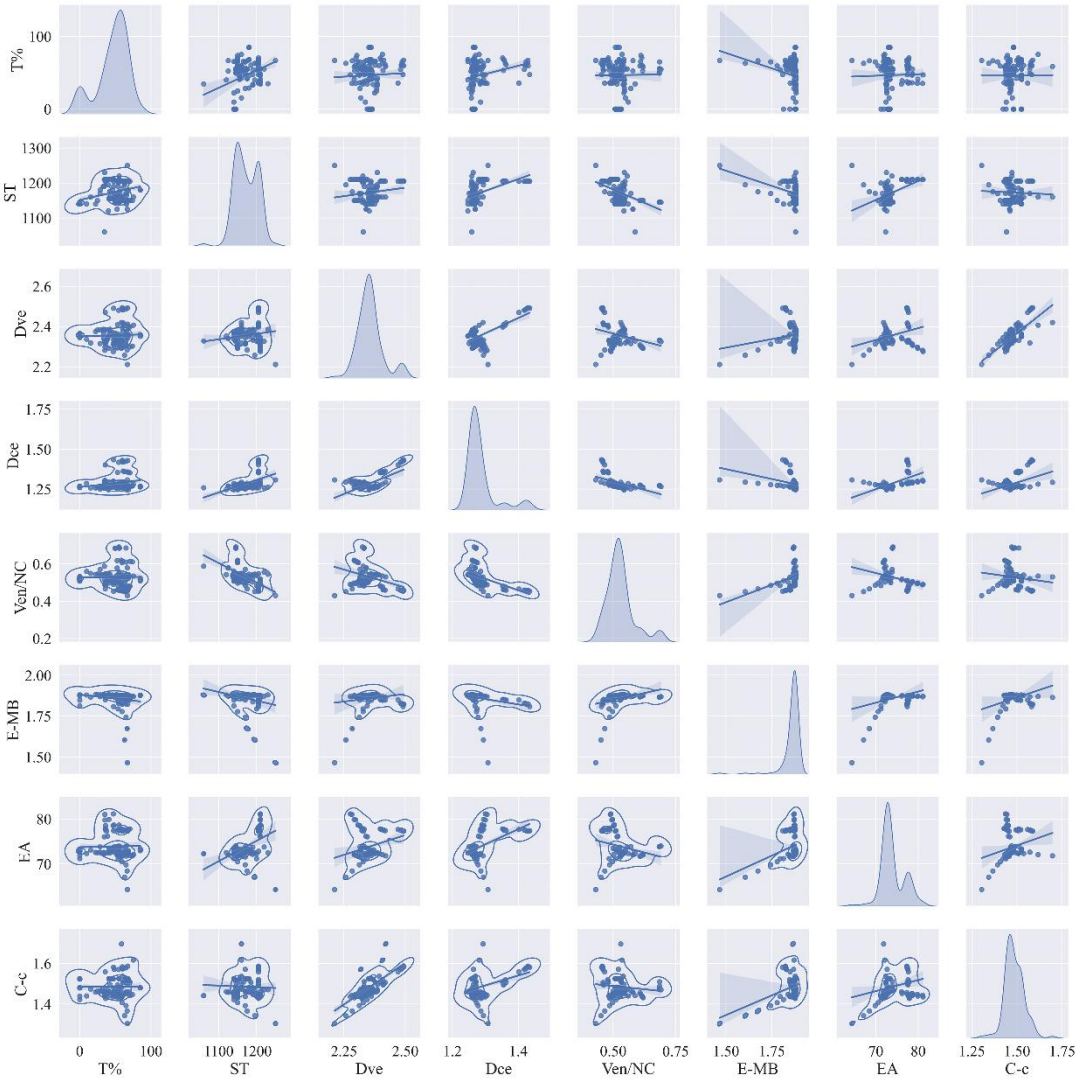

Supplementary Figure 2. Joint distribution of features in the sample data.

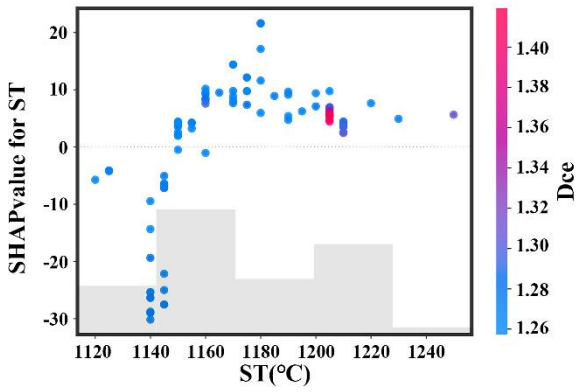

Supplementary Figure 3. SHAP dependency plot of ST and its SHAP value in ETR and Dce value mapping.

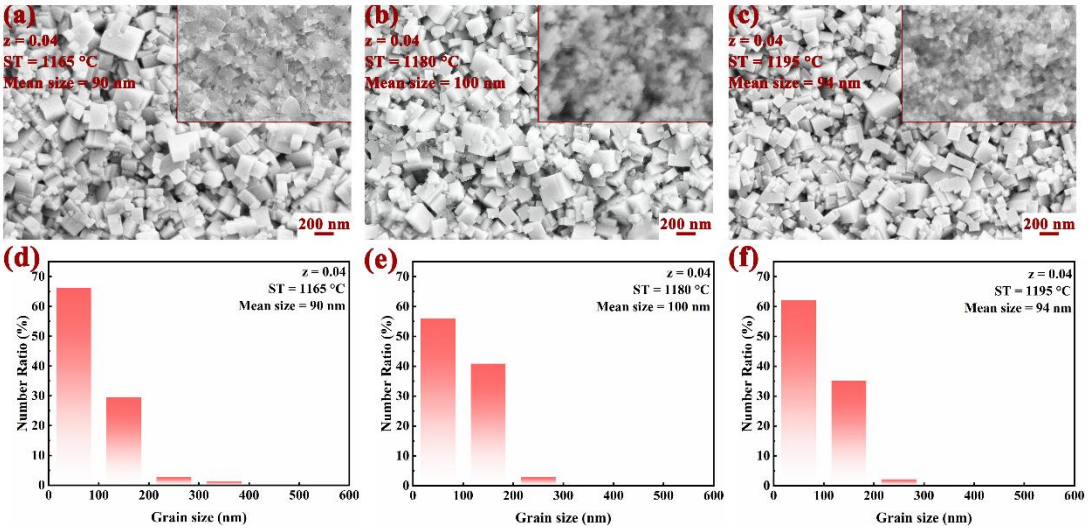

Supplementary Figure 4. SEM images of free and fractured surfaces of the 0.04Ba-0.004Tb-KNN ceramics, (a) ST = 1165 ºC, (b) ST = 1180 ºC, and (c) ST = 1195 ºC. Grain size distribution and mean size of the 0.04Ba-0.004Tb-KNN ceramics, (d) ST = 1165 ºC, (e) ST = 1180 ºC, (f) ST = 1195 ºC.

Reference

1. Russian Academy of Sciences A.A.Baikov Institute of Metallurgy and Materials Science Database on Properties of Chemical Elements, Available from: https://phases.imet-db.ru/elements/main.aspx [Last accessed 2022-06-11].

2. R D, Shannon. Revised effective ionic radii and systematic studies of interatomic distances in halides and chalcogenides. *Acta Crystallographica* 1976;A32:751-67. [DOI: 10.1107/S0567739476001551]

3. G V, Samsonov. Handbook of the Physicochemical Properties of the Elements. USA:Springer New York, NY;1968.

4. N E, Brese. M, O'keeffe. Bond-Valence Parameters for Solids. *Acta Crystallographica* 1991;B47:192-7. [DOI: 10.1107/S0108768190011041]

5. WebElements, Available from: https://www.webelements.com [Last accessed 2022-08-19].

6. S S, Batsanov. Van der Waals Radii of Elements. *Inorganic Materials* 2001;37:871-85. [DOI: 10.1023/A:1011625728803]

7. Speight JG. Lange's handbook of chemistry. New York:McGraw-Hill, NY;2005.

8. You X. Ionic polarizability. *Chinese Science Bulletin* 1974;19:419-23. (in Chinese)

9. Feng Y, Zhang S, Sun H, Li Y, Zhun Y. Ionic polarizability. *Journal of Dalian Institute of Light Industry* 2000;19:98-101.(in Chinese)

10. Zunger A. Systematization of the stable crystal structure of allAB-type binary compounds: A pseudopotential orbital-radii approach. *Physical Review B*

1980;22:5839-72. [DOI: 10.1103/PhysRevB.22.5839]